의학박사 학위논문

Biocompatibility and Efficiency of Biodegradable Magnesium-based Plates and Screws in Fractures of Zygoma of Beagles

비글의 관골 골절에서 생분해성 마그네슘 Plates와 Screws의 생체적합성 및 효율성

2018년 8월

서울대학교 대학원

의학과 성형외과학 전공

PIAO YINGLAN

Abstract

The purpose of this study was to evaluate the biocompatibility and efficiency of biodegradable magnesium-based plates and screws (magnesium alloy implant) for fixation of zygomatic arch fractures in beagle dogs.

Methods: Plates and screws were fixed in zygomatic arch fractures in beagles. Fracture healing, degradation, and bone formation were evaluated using mechanical tests, micro computed tomography, histomorphometric analysis, and histopathological analysis to compare biodegradable magnesium alloy implants with poly -L- lactide implants

Results: The fracture line was well maintained until 26 weeks in both groups. Inflammatory reactions were not significantly increased in any of the animals. Histomorphometric results showed significantly smaller normalized implant areas and larger normalized void areas in the magnesium alloy group than in the PLLA group ($p < 0.05$). The micro CT scans also showed that the void area around the implant was greater in the

magnesium alloy group than in the control group until 26 weeks. The hydrogen gas around the magnesium implant increased at 4 and 12 weeks but showed a decrease at 26 weeks. Regarding the ultimate load, the magnesium alloy group exhibited significantly higher stiffness and structural stiffness at 4 weeks than the control group. At 12 and 26 weeks, the stiffness and structural stiffness were maintained in the magnesium alloy group. In the histopathological analysis, the number of osteoclasts was significantly higher in the magnesium alloy group than in the PLLA group at 4 weeks after fixation. The magnesium alloy group exhibited a significantly higher number of osteoblasts and extent of neovascularization than the PLLA group at 26 weeks.

Conclusion: Our results show that the magnesium alloy implant had higher strength at 4 weeks after fixation, but no significant difference was observed between the 2 groups at 12 and 26 weeks. On the basis of the histological data, we speculate that the magnesium alloy implant contributed to bone regeneration in this study. These results show the possibility of future development of magnesium alloy plates and screws for human

craniofacial fixation. However, the corrosion rate of magnesium alloys needs to be optimized.

Keywords: Beagle dog, Zygomatic arch fracture, Magnesium alloy implant, Biodegradable implant

CONTENTS

LIST OF TABLES

LIST OF FIGURES

INTRODUCTION

Since the first application of resorbable polymers in craniomaxillofacial surgery, most biodegradable fixation devices used in clinical settings have consisted of poly-lactide (PLA)-based copolymers. Various polymer-based osteosynthesis devices are commercially available, with second-generation PLA-based systems also used for craniofacial pediatric indications such as craniosynostosis [1-3]. However, implants made from these materials lack the strength as devices that require a higher load indication and have a long degradation time, causing inflammation during hydrolysis [4-7]. Furthermore, because the plate of a PLA device must be shaped using a water bath prior to surgery, they are harder to handle than titanium implants from surgeons' point of view. However, although titanium implants have high strength, they must be removed by an additional operation after fixation, as permanent fixtures are associated with skeletal growth disorders in children [8, 9]. Moreover, implants made of biodegradable materials are more appropriate for inducing osteosynthesis of

the craniomaxillofacial region [10]. Thus, a bone fixation device with high strength and biocompatibility that can replace bioresorbable material must be developed [11].

Biodegradable implants consisting of Mg alloys have been studied since the last century. However, their development has been limited owing to the accumulation of hydrogen gas in the in vivo process of Mg corrosion [12, 13]. Owing to technological advances, Mg alloy implants can now be manufactured by controlling the corrosion rate of various corrosive elements by using synthesis techniques [14]. The alloy composition of the Mg alloy implant plays an important role in the in vivo degradation of the implant. Mg–Ca alloy has been reported to have the potential as a material for biocompatible load bearing implants that are degradable and possibly osteoconductive [15]. In addition, as non-acidic degradation products, Mg implants have higher mechanical strength than PLA implants and are visible on radiographs [16]. Many studies have investigated methods to control the Mg corrosion rate, cytocompatibility, bone deposition, and growth by using Mg alloy implants in small animals [17–20].

The purpose of this study was to evaluate the biocompatibility and efficiency of Mg biodegradable implants at 4, 12, and 26 weeks after fixation of zygomatic fractures in beagle dogs.

MATERIALS AND METHODS

Materials

The plates and screws used in the Mg alloy group were made of Mg alloy with a composition of 94 wt% Mg, 5 wt% Ca, and 1 wt% Zn (Korea Institute of Science and Technology, Korea). The plates and screws used in the PLLA group were commercially available implants (Inion) made of of poly -L-lactide (PLLA). The length, width, and thickness of the 4 hole plates were 24.50, 5.00, and 1.35 mm, respectively, in the experimental group (Mg group) and 25.00, 7.20, and 1.40 mm, respectively, in the control group (PLLA group). The outer diameter of the screws was 1.7 mm in the experimental group and 2.0 mm in the control group.

Animals and operation methods

All the experiments were performed in accordance with the Seoul National University Animal Care and Use Committee guidelines (Approval no. 15-0094-S1A0). Eighteen male beagle dogs (aged 24 weeks, with an average weight of 10 ±

0.5 kg) were assigned 6 each to the 4-, 12-, and 26-week groups, and were given a week of acclimation period.

Animals were anesthetized with 0.4-mg/kg xylazine (0.4 ml; Rompun, Bayer Korea Ltd., Korea) with 10-mg/kg Zoletil (0.8 ml; Virbac Korea Ltd, Korea) through intramuscular injection. Local anesthesia was induced using 1% lidocaine injected subcutaneously. With respect to the surgical method, an excision line was designed first, which spanned approximately 4 cm to the front and back from the center of the zygomatic arch. Following the design, a No. 15 blade was used to draw the excision line up to the periosteum, and detachment was performed accordingly. Hemostatic forceps were used to thoroughly control the bleeding, and complete subperiosteal dissection was performed on the front and back sides of the zygomatic arch. Double osteotomy lines were drawn with a marking pen. To prepare the space for plate fixation, each osteotomy line was designed to be 3 cm away from the other osteotomy line, after which an oscillating saw was used to create fractures in 2 locations that spanned all layers. After placing the plate on the fracture site, bicortical holes were

drilled and sufficiently tapped. During screw fixation, the screws were fastened to the end, while making sure there was no other resistance. This was performed on 4 locations, 2 each on both sides of the fracture line, and fixation was performed on 2 locations on the fracture line by using 2 plates and 8 screws. Necrotic debris was removed by thorough irrigation, and silastic drain was temporarily placed on the surgical site to prevent postsurgical hematoma. The periosteum was sutured via 4-0 VCR, and the skin was sutured as the final step.

In all the beagles, the Mg implant (2 plates and 8 screws) was fixed on the left side, and the PLLA implant was fixed on the right side of the zygomatic arch (Figure 1).

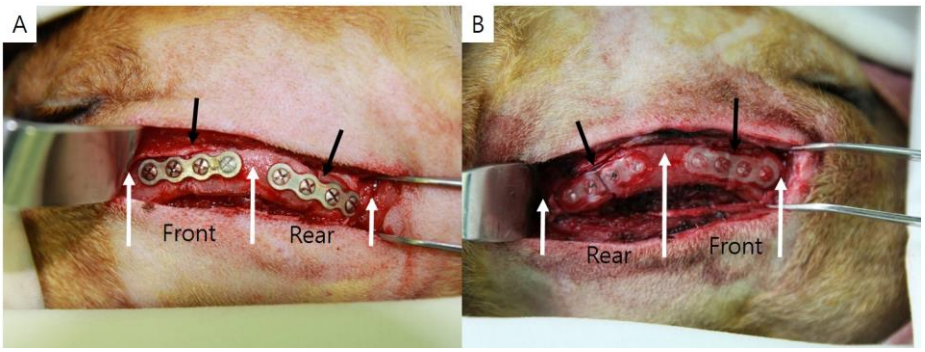

Figure 1. Operation procedure.

The plate and screw are fixated at 2 flanks of the zygomatic arch. A: Mg alloy group and B: PLLA group. The black arrows indicate the fracture lines, and the white arrows indicate the biopsy cutting lines. The anterior bone–implant complex was used for mechanical testing, and the posterior complex was used for histological analysis.

An antibiotic regimen consisting of cephazoline 20 mg/kg was intramuscularly administered twice daily for 5 days, while meloxicam 0.4 ml/kg was administered for 5 days for pain control. The surgical site was dressed with betadine solution for 5 days to keep the site clean and to prevent infections. Blood samples were collected at 4, 12, and 26 weeks Postoperative from both the Mg alloy and PLLA groups. Thereafter, the beagle dogs belonging to each group with different numbers of weeks were sacrificed accordingly. Then, radiographs were taken, and bone segments were harvested, with the segment from the front used for micro CT imaging and mechanical testing, and the segment from the back used for histopathological and histomorphometric analyses.

Blood testing

For all the groups, biochemistry, complete blood count, and blood coagulation test were performed before surgery and before sacrifice to clarify whether Mg alloys had any harmful effects.

Radiographic and Micro-CT examination

Radiographs of the head (anteroposterior and lateral views) were performed after 3, 7, and 14 days, and just prior to sacrifice, with a C-arm machine (Philipps BV Pulsera) and with the animals under short general anesthesia. Radiographic examinations were performed to monitor the implant location, integrity, and gas formation.

For accurate identification of the degree of bone healing, bone specimens were imaged using an ex vivo micro CT device (SkyScan1172, Belgium). Surface reconstruction was performed on the acquired images by using a N-Recon program (SkyScan). Surface reconstructed images were reconstructed into three-dimensional images (coronal, sagittal, and horizontal views) by using a data viewer program (SkyScan), after which the shape images of the fixed plates and screws were analyzed using their horizontal view images.

Mechanical testing

To determine the ultimate load and structural stiffness, we used a 3-point bending test to evaluate the strength of the bone implant complex. As shown in the figure, the loading span (diameter: 3 mm) was positioned to be completely seated on the surface of the specimen. The rigid extension is connected to the 2 tips of the bone plate complex. Mechanical tests were performed using a 2.5-ton MTS machine (MTS, Eden Prairie, MN) at 20°C ± 40% humidity. The loading span was adjusted to be positioned in the middle because the specimens to be tested were not completely symmetrical relative to the central axis. Moreover, caution was taken to make sure the loading span did not come in contact with the screw holes in the plate. A load-displacement curve was drawn with a load of 5 mm/min [21]. (Figure 2)

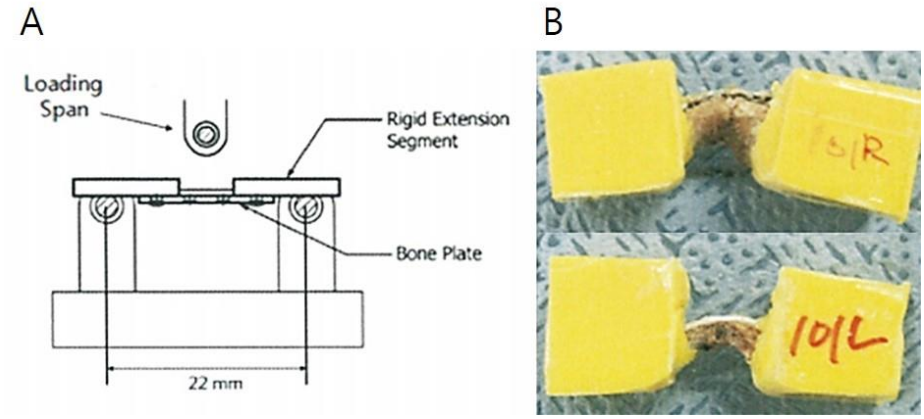

Figure 2. Mechanical test methods. A: The 3-point mechanical bending test. B: Bone-implant complex center after the mechanical test. (Upper panel: experimental group and lower panel: control group.)

Histologic analysis

For histomorphometric analysis, the plastic-embedded slides were dyed using 0.5% toluidine blue after decalcification (3 times at 15 min each) with 2-methoxyethyl acetate.

Images of the bone tissue around the implant were obtained with the cellSens Standard software (Olympus, Tokyo, Japan) to analyze its structure and shape. The total defect, bone, implant, soft tissue, and void areas were measured using i-Solution (Innerview, Seongnam, Korea). To normalize the values, each value was converted to a relative percentage of the total defect area (100%).

Each slide specimen was histopathologically evaluated using the Histopathology Evaluation System for Cell Type/Response in ISO 10993 as a reference. The evaluation items and scoring standards are shown in Table 1.

Cell Type / Response	Score				
	0	1	2	3	4
Polymorphonuclear cells	None	Rare, 1-5/phf*	5-10/phf	Heavy infiltrate	Packed
Lymphocytes	None	Rare, 1-5/phf	5-10/phf	Heavy infiltrate	Packed
Plasma cells	None	Rare, 1-5/phf	5-10/phf	Heavy infiltrate	Packed
Macrophages	None	Rare, 1-5/phf	5-10/phf	Heavy infiltrate	Packed
Multinucleated giant cells	None	Rare, 1-2/phf	3-5/phf	Heavy infiltrate	Sheets
Necrosis	None	Minimal	Mild	Moderate	Severe
Osteoblastic cells	Severe	Moderate	Mild	Minimal	None
Signs of bone remodeling by osteoclasts	Severe	Moderate	Mild	Minimal	None
Neovascularization	Severe	Moderate	Mild	Minimal	None
Fibrosis	None	Narrow band	Moderately thick band	Thick band	Extensive band
Fatty infiltrate	None	Minimal amount of fat associated with fibrosis	Several layers of fat and fibrosis	Elongated and broad accumulation of fat cells about the implant site	Extensive fat completely surrounding the implant
Signs of graft dissolution / degradation	None	Minimal	Mild	Moderate	Severe
Bone debris	None	Minimal	Mild	Moderate	Severe
** phf – per high powered (400 x) field*					

Table 1. Histopathology Evaluation System for Cell Type/Response (ISO 10993)

Statistical analysis

For determination of significant differences in measurements between the experimental and control groups, the Wilcoxon signed-rank test (SPSS version 23, IBM, Armonk, NY), which takes into account-matched data, was performed. The Mann-Whitney test was used to evaluate the significant difference in mechanical test results between the 2 groups. A p value of <0.05 was considered to indicate statistical significance.

RESULTS

Postoperative observation

Overall, most of the animals ate well and were active after the surgery. The surgical sites were well sutured on the outside, the swelling subsided after 3–4 days, and both sides of the surgical site were symmetrical. The surgical wounds healed well without substantial complications, except for wound dehiscence and mild inflammation in 2 beagles from each group (4−, 12−, and 26−week groups; total of 6 beagles). These were observed above the periosteum layer and treated with conservative management, including prolonged use of antibiotics, wound revision, and dressing. No significant difference in inflammatory response was observed between the experimental and control groups. Afterward, the surgical wounds remained well until the animals were sacrificed at 4, 12, and 26 weeks postoperatively.

Blood test examination revealed no statistically significant difference between before and after surgery in the 4−, 12−,

and 26-week groups [22-24]. As the implants of the experimental and control groups were fixed on each side of the zygoma arch of each dog, the blood test can only evaluate the changes before and after surgery. When compared between before and after surgery, the inflammatory markers such as the lymphocyte, eosinophil, and neutrophilic leukocyte counts were not significantly increased (Table 2).

Blood test	Referensce range	4 weeks		12 weeks		26 weeks	
		Pre-op	Post-op	Pre-op	Post-op	Pre-op	Post-op
WBC	5.4-15.3	11.03±2.92	9.94±1.40	11.03±2.63	10.22±2.80	11.85±1.62	11.00±1.09
PLT	268-386.6	259.50±84.86	263.67±73.07	343.67±66.28	252.33±99.25	248.17±98.02	308.67±51.45
NEUT	3-11.4	6.47±2.18	5.81±0.68	6.23±1.93	6.36±1.88	7.60±1.75	6.82±0.84
NEUT%	60-70%	57.37±7.67	58.85±5.15	55.90±8.40	61.98±2.42	63.43±6.36	62.05±4.29
LYMPH	1-4.8	3.60±0.79	3.18±0.83	3.68±0.87	3.09±0.78	3.19±0.57	3.29±0.49
LYMPH%	10.87-46.67	33.88±7.49	31.70±4.93	33.82±5.12	30.38±1.33	27.60±6.34	29.97±4.08
EOS	0.1-0.75	0.27±0.13	0.25±0.08	0.33±0.19	0.21±0.05	0.22±0.12	0.27±0.08
EOS%	2-10%	2.50±0.89	2.48±0.70	3.02±1.76	2.22±0.64	1.85±0.91	2.50±0.70
Mg	1.7-2.7	1.74±0.16	1.71±0.13	1.67±0.12	1.78±0.19	1.82±0.18	1.99±0.18
Ca	8.4-11.6	8.85±0.71	7.43±0.58	7.58±0.53	8.92±1.88	9.20±0.51	10.77±0.61
IP	2.68-7.68	5.80±0.89	7.08±0.63	5.52±0.93	5.68±0.46	7.27±0.51	6.20±0.76
GLU	87-323	111.17±13.17	103.33±7.63	114.50±11.46	106.50±18.20	108.33±13.60	85.00±18.20
BUN	7~26	15.12±3.79	13.00±2.00	14.02±5.01	14.32±3.88	12.83±2.98	17.95±4.23
CRE	0.61-2.45	0.68±0.07	0.74±0.06	0.73±0.08	0.81±0.10	0.77±0.12	0.82±0.09
ALB	2.1-3.8	2.90±0.23	2.77±0.18	2.93±0.05	2.73±0.09	3.08±0.09	2.68±0.16
AST	28.69-39.79	34.17±9.46	35.17±6.41	41.00±4.58	33.50±5.77	34.17±8.41	38.67±10.48
ALT	8.2-57	34.00±13.74	36.00±8.87	43.33±6.47	46.17±9.41	20.50±4.19	40.00±18.30
Na	123-147	146.70±1.90	145.47±3.10	143.03±1.93	149.50±1.71	141.32±1.54	145.00±2.38
K	2.8-6	4.87±0.20	4.17±0.36	4.49±0.26	4.83±0.91	5.87±1.49	6.03±0.95
Cl	98-115	105.98±2.62	105.48±2.33	101.62±1.80	113.50±1.12	113.18±1.92	121.00±4.47
coagulation_PT	6~10	9.01±2.61	7.53±0.98	7.75±0.59	6.58±0.45	8.17±1.34	7.10±0.65
coagulation_aPTT	11~19	21.18±5.93	14.70±2.32	17.87±2.91	13.50±1.63	21.52±5.28	15.38±1.53

Table 2. Blood test results.

Blood test examination revealed no statistically significant difference between before and after surgery in the 4-, 12-, and 26-week groups.

Radiographic evaluation and Micro-CT analysis

The Mg plates and screws were clearly visible radiologically as compared with the PLLA plates and screws. No abnormal findings were obtained in all the groups, indicating displacement of the bone segments or fractures.

The radiographs showed larger void areas around the implant in the Mg alloy group than in the control group (Figure 3). The CT scans obtained at 24 days after surgery showed clearer void areas around the implant in the experimental group than in the control group (Figure 4).

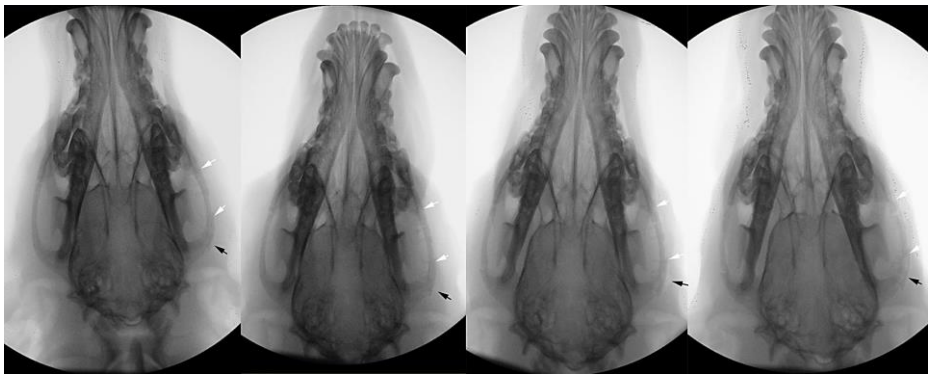

FIGURE 3. Simple radiographs taken 3, 7, and 14 days and 4 weeks after Mg alloy fixation. The white arrows indicate the Mg alloy implant, and the black arrows indicate air pockets.

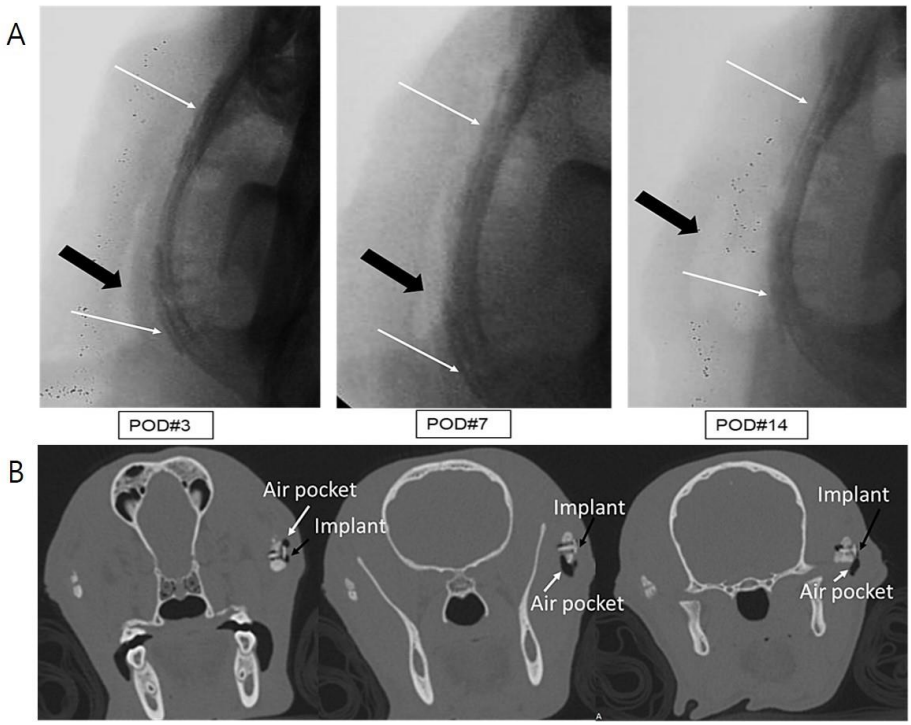

FIGURE 4. A: Magnified radiographs taken 3, 7, and 14 days after Mg alloy fixation. The white arrows indicate the Mg alloy implant, and the black arrows indicate air pockets. B: CT scans obtained at 24 days after surgery, showing void areas (white arrow) around the Mg alloy implant (black arrow).

Figures 5 and 6 show the micro CT scans of the implant in the coronal and horizontal views. The experimental group showed a larger void areas distribution around the screw than the control group until 26 weeks. The normalized total defect, remaining implant, bone, and void areas were histologically measured and analyzed.

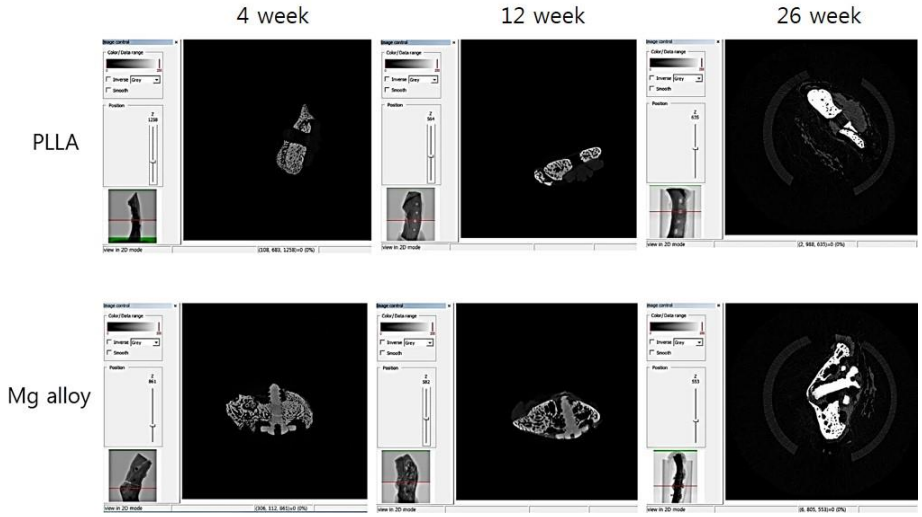

FIGURE 5. Micro CT scans of the implant in the coronal view. The Mg plates and screws are clearly visible on the micro CT scans, as compared with the PLLA plates and screws.

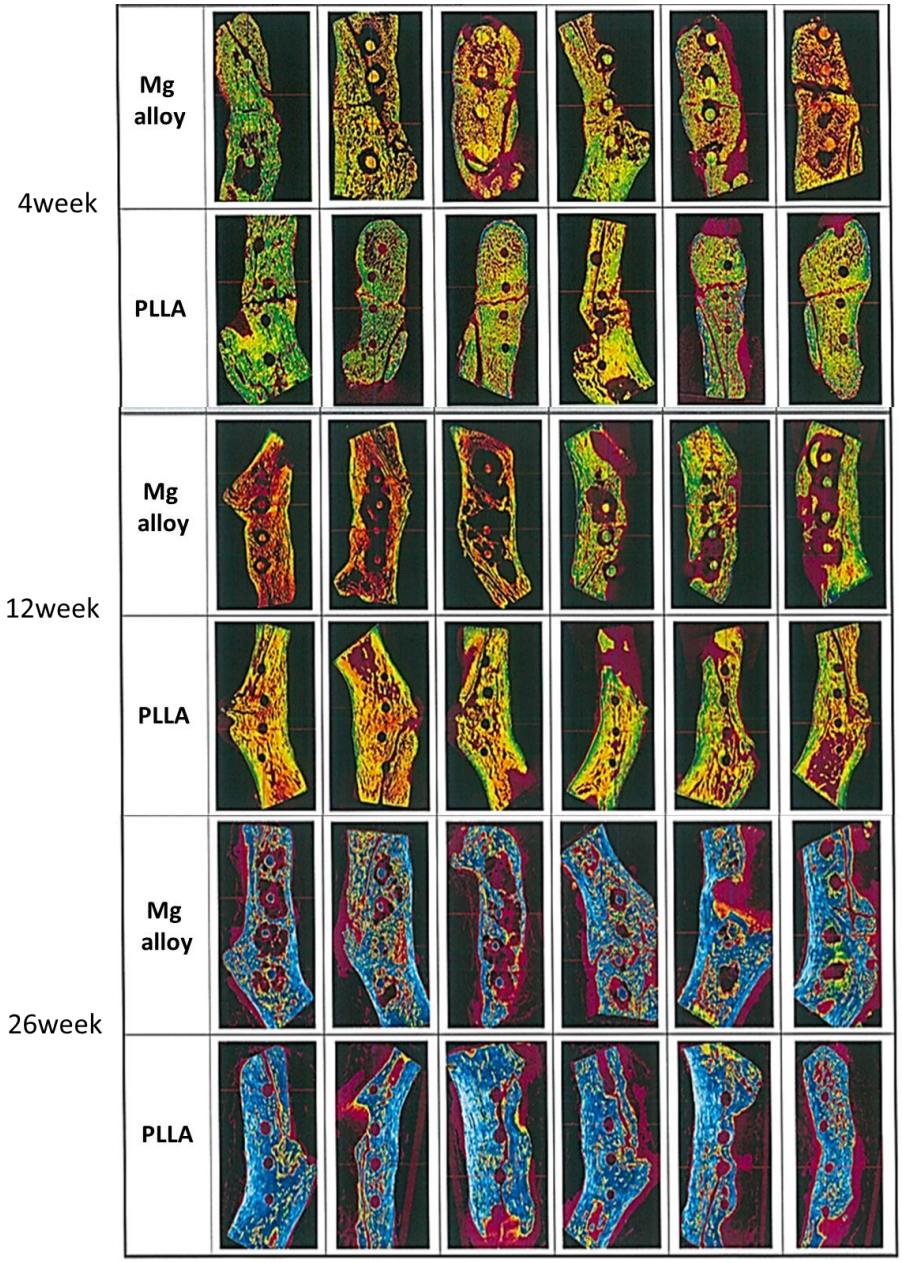

FIGURE 6. Micro CT scans of the implant in the horizontal view.

Mechanical testing

The ultimate loads (the maximal loads bone plates can bear before failure) measured at 4, 12, and 26 weeks were respectively 241.4 ± 96.0, 184.9 ± 47.2, and 249.5 ± 150.0 N in the magnesium alloy group and 100.9 ± 89.8, 293.6 ± 92.4, and 351.1 ± 99.0 N in the control group.

The structural stiffness values (ultimate load per unit area) measured at 4, 12, and 26 weeks were respectively 36,417.3 ± 11,761.9, 19,792.5 ± 16,852.8, and 18,135.4 ± 42,93.1 N/mm^2 in the magnesium alloy group and 17,678.2 ± 11,638.9, 42,321.1 ± 23,070.0, and 27,589.8 ± 13,328.3 N/mm^2 in the control group (Figures 7).

The ultimate load and structural stiffness were significantly different between the 2 groups only at 4 weeks ($p < 0.05$). At 12 and 26 weeks, the implants in the magnesium alloy group maintained their stiffness and structural stiffness, and no

significant difference was found between the 2 groups at 12 and 26 weeks.

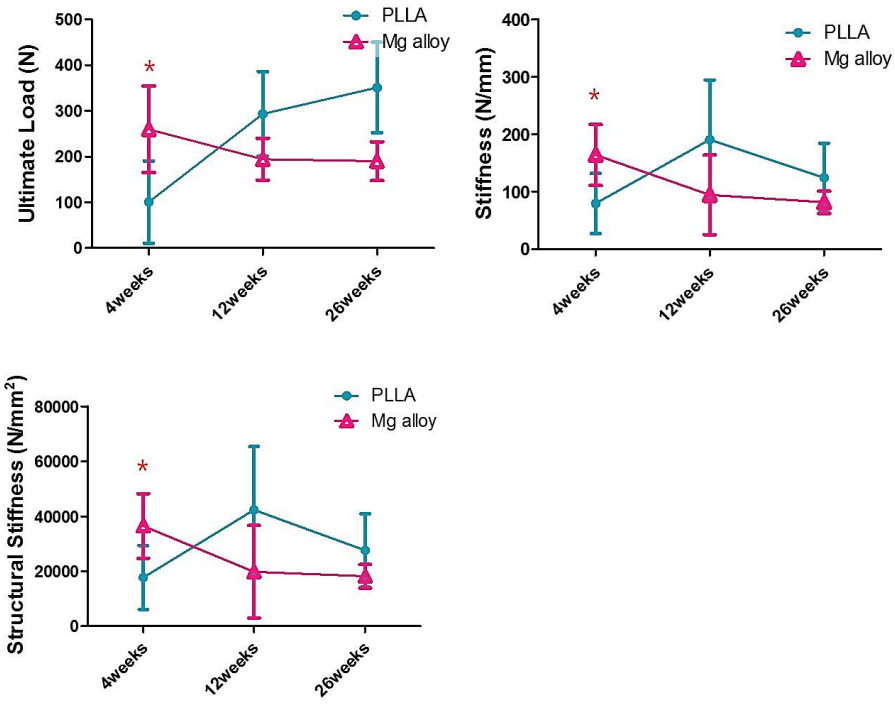

FIGURE 7. Mechanical test analysis.

The average and statistical significance of the ultimate load, stiffness, and structural stiffness of the Mg alloy and PLLA groups. The mechanical test results of the bone–implant complex in the 4–, 12–, and 26–week groups. $*p < 0.05$.

Histological evaluation

The Mg alloy group showed significantly smaller normalized implant areas and larger normalized void areas than the PLLA group ($p < 0.05$). The normalized implant areas were 35.6% ± 14.1% (4 weeks), 32.3% ± 15.1% (12 weeks), and 26.2% ± 10.3% (26 weeks) in the Mg alloy group and 54.1% ± 24.9% (4 weeks), 86.2% ± 15.2% (12 weeks), and 78.5% ± 11.3% (26 weeks) in the control group.

The normalized void areas were 37.1% ± 11.9% (4 weeks), 41.5% ± 11.6% (12 weeks), and 35.4% ± 8.4% (26 weeks) in the Mg alloy group and 12.9% ± 7.9% (4 weeks), 2.5% ± 3.4% (12 weeks), and 6.3% ± 8.4% (26 weeks) in the control group (Figures 8 and 9). The normalized bone and soft tissue areas are shown in Table 3.

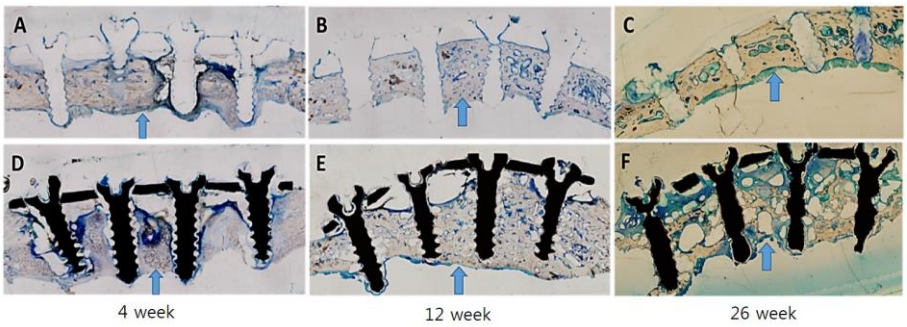

FIGURE 8. Characteristics of Toluidine blue staining.

Thin histological thin slides of PLLA (A–C) and Mg alloy (D–F) plates and screws (image magnification x12.5). The arrows indicate the fracture lines.

		Normalized implant area %	Normalized bone area %	Normalized soft tissue area %	Normalized void area %
4week	**PLLA**	54.1±24.9	2.9±3.4	30.1±21.4	12.9±7.9
	Mg alloy	35.6±14.1	6.3±3.5	21.0±10.7	37.1±11.9
12week	**PLLA**	86.2±15.2	1.3±2.7	10.1±15.3	2.5±3.4
	Mg alloy	32.3±15.1	14.5±3.2	11.7±6.2	41.5±11.6
24week	**PLLA**	78.5±11.3	0.3±0.3	15.0±14.5	6.3±8.4
	Mg alloy	26.2±10.3	12.6±2.2	25.8±3.8	35.4±8.4

Table 3. Histomorphometric assessment of the normalized area (%) in the Mg alloy and PLLA groups. To normalize the values, each value was converted to a relative percentage of the total defect area (100%).

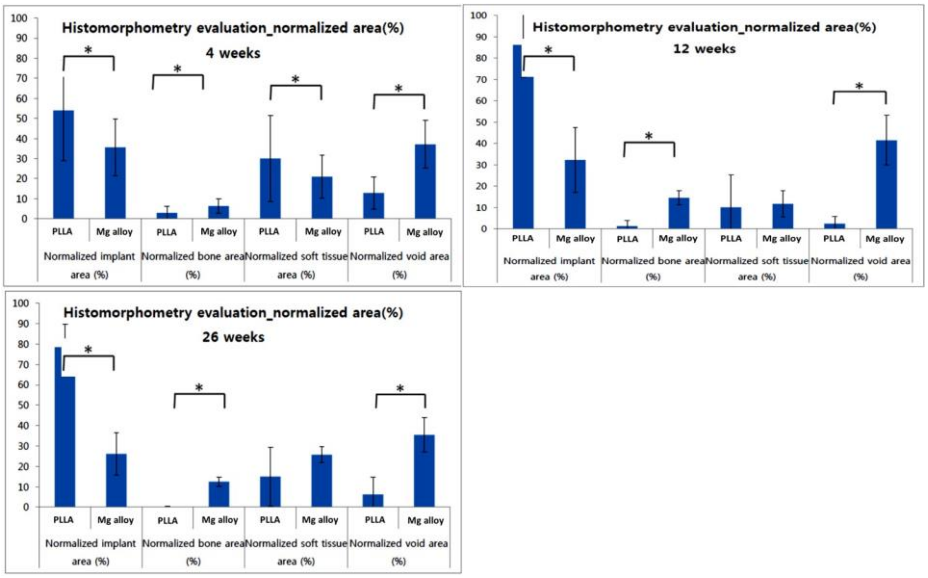

FIGURE 9. Histomorphometric analysis using i-Solution to measure the total defect, bone, implant, soft tissue, and void areas. $*p < 0.05$.

.

The scores for the osteoblastic cells and neovascularization, which are related to a new bone formation activity, were relatively lower in the Mg alloy group than in the PLLA group at 26 weeks ($p < 0.05$). The scores for the signs of bone remodeling by osteoclasts was relatively lower in the Mg alloy group than in the control group at 4 weeks ($p < 0.05$). A lower score means higher new bone formation activity (Figures 10 and 11).

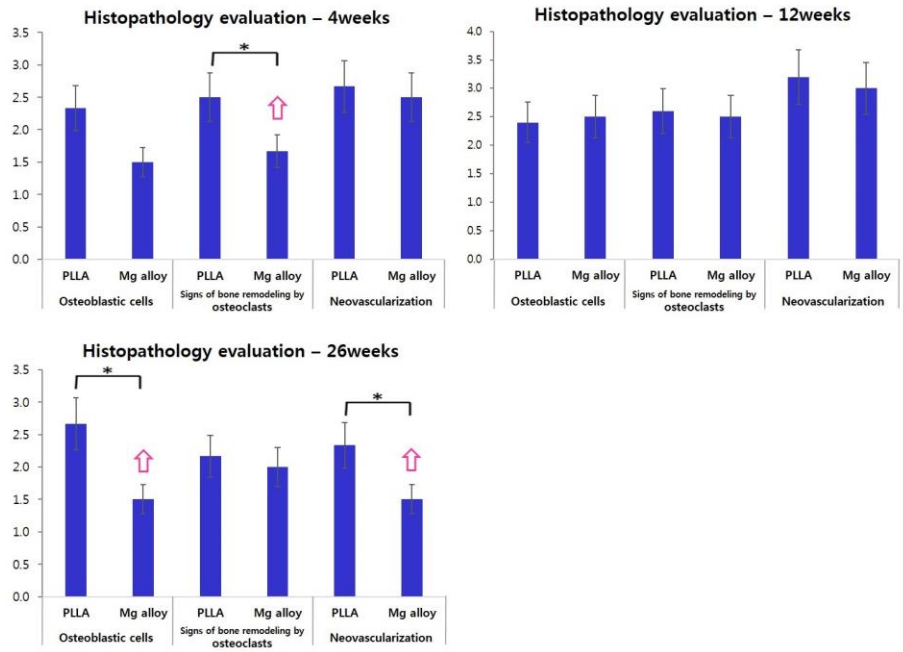

FIGURE 10. Histopathology evaluation (osteoblastic cells, signs of bone remodeling by osteoclasts, and neovascularization) for the 4−, 12−, and 26−week groups. $*p < 0.05$.

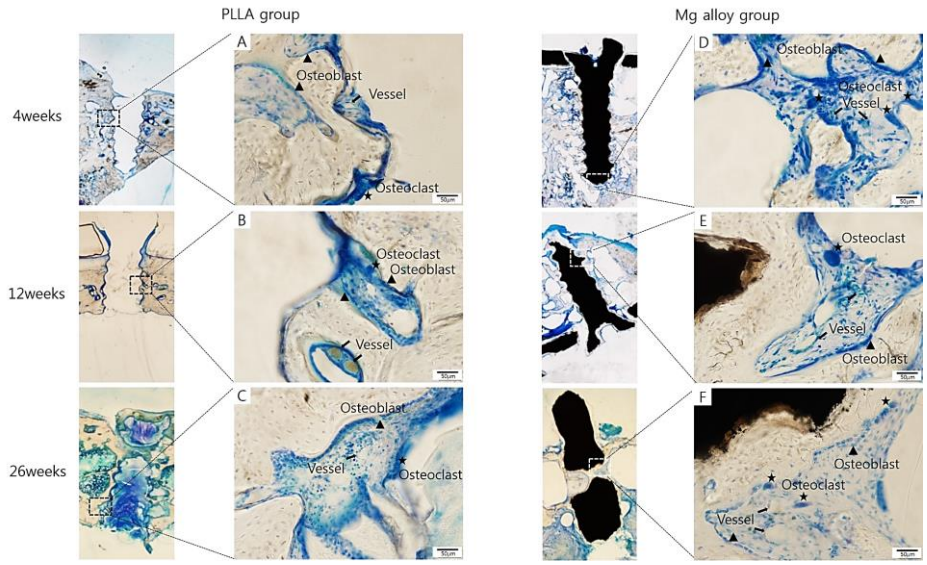

FIGURE 11. Histopathological images showing increased cellular activity related to neo-osteogenesis in the PLLA and Mg alloy groups (toluidine blue staining, original magnification 200). The triangle indicates the osteoblast, the arrow indicates the blood vessel, and the asterisk indicates the osteoclast.

DISCUSSION

Magnesium is a light metal essential for metabolism. Its biodegradable capacity in vivo has been widely applied in clinical situations such as cardiovascular stents and orthopedic surgery [25]

Previous studies confirmed that Mg-Ca-Zn is not cytotoxic and has good tissue compatibility in a rabbit model of femoral condyle fracture [26]. A recent clinical study showed that Mg-Ca-Zn screws facilitated early bone healing and were replaced with new bone at 1 year after fixation [27]. However, to the best of our knowledge, no study has clarified the effects of human standard-sized plates and screws in large-animal facial fractures. The present study was designed to evaluate the biocompatibility and efficacy of magnesium-based plates in adult facial bone fractures. The masseter muscle receives the greatest load of all the muscles in the oral and maxillofacial region. The amount of force that is momentarily applied upon chewing in humans is approximately 450 N, and beagles are reported to have a similar force of approximately 500 N [28,

29]. Beagles were selected as the appropriate animals for this study, as they have a zygomatic arch of sufficient length, which would enable fixation of 2 plates and screws on one side of the zygomatic arch.

In our study, wound dehiscence and mild inflammation were observed in 2 beagles from each group (4−, 12−, and 26−week groups, total of 6 beagles). We believe the wound problem had little relationship to the plates and screws because the wound was shallow, with the periosteum remaining intact above the plates. We speculate two possible reasons for the occurrence of the complications, namely that the beagle dogs ingested food and uncontrollably touched their wounds.

The histopathological results showed no significant difference in the distribution or number of inflammatory cells between the 2 groups. In addition, laboratory tests revealed no increase in inflammatory markers. More new bone formation activities were observed in the Mg alloy group. The increase in osteoclast activity at 4 weeks showed early bone healing and old bone resorption to make space for new bone. At 26 weeks,

more osteoblasts and increased neovascularization also demonstrated new bone formation. The polymer plates and screws used in the control group have been reported to show bulk erosion through a hydrolysis mechanism [30]. Thus, they maintain their original outlines with few morphological changes over time after implantation. They begin to degrade 1 year after implantation and can require >2 years before they are completely absorbed biologically [21]. The indwelling of screws for longer than the initially required period for bone healing might not provide osteoconductive property during its degradation process. It can cause foreign body reactions, inflammation, and wound problems [4, 7].

Histomorphometric measurement performed at the bone–implant interspace showed relatively smaller implant area and larger void area in the Mg alloy group. This shows the corrosion of the Mg alloy inside the body immediately after fixation. In our histological study, the new bone forms direct contact with the material and around the gas voids. Therefore, magnesium itself seems to be biocompatible. However, over time, the accumulated byproduct creates mechanical barriers

for the cells surrounding the implant.[31]. Early corrosion of the magnesium screws could explain this phenomenon. The effect of byproducts, including hydrogen gas, on the resorption of surrounding bone might be another explanation. Previous studies demonstrated bone resorption from hydrogen gas when magnesium was implanted in vivo [32, 33]

The nature of magnesium degradation is associated with hydrogen gas evolution, which forms gas cavities in the surrounding tissue [32, 34]. Magnesium degrades in vivo via the following corrosion reaction: $Mg + 2H_2O \rightarrow Mg(OH)_2 + H_2$. . A large amount of hydrogen gas accumulates in the tissue cavity [16, 35]. A study has shown that while the alloy discs are constantly corroded and the size of the cavity increases, the evolving H2 of the growing cavity is continuously exchanged with dissolved gases such as N_2, O_2 and CO_2 in neighboring tissues and blood vessels[36].

The accumulation of hydrogen is related to factors such as magnesium content in the adjacent tissues, osmotic pressure, acidity, and manufacturing methods [37, 38]. The alloying of

most elements such as aluminum and zinc increases the oxidation rate, while the alloying of magnesium and rare earth elements reduces the oxidation rate of magnesium alloys [16, 26]. However, the coating did not prevent magnesium degradation [39, 40]. The effect of excessive gas in cavities has not been determined yet. In this study, the Mg alloy group showed unsatisfactory results in the mechanical strength test as compared with the control group. The mechanical strength was lower in the Mg alloy group than the control group at 12 and 26 weeks. However, the Mg alloy group showed higher strength than the control group at 4 weeks. Therefore, magnesium alloys seem to provide sufficiently high strength in the early stages of fracture. Although the optimal duration of mechanical support for bone fixation differs according to the clinical condition and individual compliance, 4 to 8 weeks was an adequate duration to provide initial strength after fracture reduction in humans.

On the other hand, osteoclasts absorb osteons and form absorption cavities for the ingrowth of new vessels and osteoblasts [41]. Increased absorption cavities generated by

osteoclasts around the Mg implant may increase the void area. Previous studies reported that the void area was replaced by new bone formation [16, 27]. This may explain the void area measured after 26 weeks of fixing Mg alloy in our study, which was <12 weeks. Future studies must investigate methods to optimize the corrosion rate of Mg alloys and minimize hydrogen gas formation.

CONCLUSION

Our results showed that the Mg alloy had higher strength at 4 weeks after fixation but no significant difference between the 2 groups at 12 and 26 weeks. On the basis of the histological data, we speculate that the Mg alloy implant contributed to bone regeneration in this study. These results show the possibility of future development of magnesium alloy plates and screws for human craniofacial fixation. However, the corrosion rate of magnesium alloys needs to be optimized.

REFERENCES

1. Suuronen, R., et al., *Bioabsorbable self-reinforced plates and screws in craniomaxillofacial surgery.* Biomed Mater Eng, 2004. **14**(4): p. 517-24.
2. Guzman, R., et al., *Fronto-orbital advancement using an en bloc frontal bone craniectomy.* Neurosurgery, 2011. **68**(1 Suppl Operative): p. 68-74.
3. Hayden Gephart, M.G., et al., *Using bioabsorbable fixation systems in the treatment of pediatric skull deformities leads to good outcomes and low morbidity.* Childs Nerv Syst, 2013. **29**(2): p. 297-301.
4. Bergsma, J.E., et al., *Late degradation tissue response to poly(L-lactide) bone plates and screws.* Biomaterials, 1995. **16**(1): p. 25-31.
5. Bostman, O., et al., *Foreign-body reactions to fracture fixation implants of biodegradable synthetic polymers.* J Bone Joint Surg Br, 1990. **72**(4): p. 592-6.
6. Rha, E.Y., H. Paik, and J.H. Byeon, *Bioabsorbable plates and screws fixation in mandible fractures: clinical retrospective research during a 10-year period.* Ann Plast Surg, 2015. **74**(4): p. 432-6.
7. Weiler, A., et al., *Foreign-body reaction and the course of osteolysis after polyglycolide implants for fracture fixation: experimental study in sheep.* J Bone Joint Surg Br, 1996. **78**(3): p. 369-76.
8. Busam, M.L., R.J. Esther, and W.T. Obremskey, *Hardware removal: indications and expectations.* J Am Acad Orthop Surg, 2006. **14**(2): p. 113-20.
9. Puleo, D.A. and W.W. Huh, *Acute toxicity of metal ions in cultures of osteogenic cells derived from bone marrow stromal cells.* J Appl Biomater, 1995. **6**(2): p. 109-16.
10. Thoren, H., et al., *Policy of routine titanium miniplate removal after maxillofacial trauma.* J Oral Maxillofac Surg, 2008. **66**(9): p. 1901-4.
11. Schumann, P., et al., *Perspectives on resorbable osteosynthesis materials in craniomaxillofacial surgery.* Pathobiology, 2013. **80**(4): p.

211-7.

12. Thormann, U., et al., *The biocompatibility of degradable magnesium interference screws: an experimental study with sheep.* Biomed Res Int, 2015. **2015**: p. 943603.
13. Dorozhkin, S.V., *Calcium orthophosphate coatings on magnesium and its biodegradable alloys.* Acta Biomaterialia, 2014. **10**(7): p. 2919-2934.
14. James, J., *Recent advancements in magnesium implants for orthopedic application and associated infections.* Clinical Trials in Orthopedic Disorders, 2016. **1**(4): p. 138-144.
15. Han, H.-S., et al., *Bone formation within the vicinity of biodegradable magnesium alloy implant in a rat femur model.* Metals and Materials International, 2012. **18**(2): p. 243-247.
16. Witte, F., et al., *In vivo corrosion of four magnesium alloys and the associated bone response.* Biomaterials, 2005. **26**(17): p. 3557-63.
17. Rzeszotarski, P. and Z. Kaszkur, *Surface reconstruction of Pt nanocrystals interacting with gas atmosphere. Bridging the pressure gap with in situ diffraction.* Phys Chem Chem Phys, 2009. **11**(26): p. 5416-21.
18. Schaller, B., et al., *In vivo degradation of magnesium plate/screw osteosynthesis implant systems: Soft and hard tissue response in a calvarial model in miniature pigs.* J Craniomaxillofac Surg, 2016. **44**(3): p. 309-17.
19. Thaller, S.R., V. Huang, and H. Tesluk, *Use of biodegradable plates and screws in a rabbit model.* J Craniofac Surg, 1992. **2**(4): p. 168-73.
20. Zhang, Z., et al., *[The experimental study of bioabsorbable mini-plate for rigid fixation on rabbits].* Zhonghua Zheng Xing Wai Ke Za Zhi, 2002. **18**(1): p. 38-40.
21. Nieminen, T., et al., *Degradative and mechanical properties of a novel resorbable plating system during a 3-year follow-up in vivo and in vitro.* J Mater Sci Mater Med, 2008. **19**(3): p. 1155-63.

22. Brunk, R.R., *Standard values in the beagle dog: haematology and clinical chemistry.* Food Cosmet Toxicol, 1969. **7**(2): p. 141-8.
23. Choi, S.Y., et al., *Basic data on the hematology, serum biochemistry, urology, and organ weights of beagle dogs.* Lab Anim Res, 2011. **27**(4): p. 283-91.
24. Ikeuchi, J., T. Yoshizaki, and M. Hirata, *Plasma biochemistry values of young beagle dogs.* J Toxicol Sci, 1991. **16**(2): p. 49-59.
25. Windhagen, H., et al., *Biodegradable magnesium-based screw clinically equivalent to titanium screw in hallux valgus surgery: short term results of the first prospective, randomized, controlled clinical pilot study.* Biomed Eng Online, 2013. **12**: p. 62.
26. Cha, P.R., et al., *Biodegradability engineering of biodegradable Mg alloys: tailoring the electrochemical properties and microstructure of constituent phases.* Sci Rep, 2013. **3**: p. 2367.
27. Lee, J.W., et al., *Long-term clinical study and multiscale analysis of in vivo biodegradation mechanism of Mg alloy.* Proc Natl Acad Sci U S A, 2016. **113**(3): p. 716-21.
28. Christiansen, P. and S. Wroe, *Bite forces and evolutionary adaptations to feeding ecology in carnivores.* Ecology, 2007. **88**(2): p. 347-58.
29. Strom, D. and S. Holm, *Bite-force development, metabolic and circulatory response to electrical stimulation in the canine and porcine masseter muscles.* Arch Oral Biol, 1992. **37**(12): p. 997-1006.
30. Nair, L.S. and C.T. Laurencin, *Biodegradable polymers as biomaterials.* Progress in Polymer Science, 2007. **32**(8): p. 762-798.
31. Charyeva, O., et al., *Histological Comparison of New Biodegradable Magnesium-Based Implants for Maxillofacial Applications.* Journal of Maxillofacial and Oral Surgery, 2015. **14**(3): p. 637-645.
32. Kuhlmann, J., et al., *Fast escape of hydrogen from gas cavities around corroding magnesium implants.* Acta Biomater, 2013. **9**(10): p. 8714-21.
33. Luthringer, B.J., F. Feyerabend, and R. Willumeit-Romer, *Magnesium-*

based implants: a mini-review. Magnes Res, 2014. **27**(4): p. 142-54.

34. Kraus, T., et al., *Magnesium alloys for temporary implants in osteosynthesis: in vivo studies of their degradation and interaction with bone.* Acta Biomater, 2012. **8**(3): p. 1230-8.
35. Witte, F., et al., *In vivo corrosion and corrosion protection of magnesium alloy LAE442.* Acta Biomater, 2010. **6**(5): p. 1792-9.
36. Kety, S.S., *The theory and applications of the exchange of inert gas at the lungs and tissues.* Pharmacol Rev, 1951. **3**(1): p. 1-41.
37. Martinez Sanchez, A.H., et al., *Mg and Mg alloys: how comparable are in vitro and in vivo corrosion rates? A review.* Acta Biomater, 2015. **13**: p. 16-31.
38. Staiger, M.P., et al., *Magnesium and its alloys as orthopedic biomaterials: a review.* Biomaterials, 2006. **27**(9): p. 1728-34.
39. Thomann, M., et al., *Influence of a magnesium-fluoride coating of magnesium-based implants (MgCa0.8) on degradation in a rabbit model.* J Biomed Mater Res A, 2010. **93**(4): p. 1609-19.
40. Keim, S., et al., *Control of magnesium corrosion and biocompatibility with biomimetic coatings.* J Biomed Mater Res B Appl Biomater, 2011. **96**(1): p. 84-90.
41. Claes, L., S. Recknagel, and A. Ignatius, *Fracture healing under healthy and inflammatory conditions.* Nat Rev Rheumatol, 2012. **8**(3): p. 133-43.

국문 초록

본 연구의 목적은 Magnesium-based plate & screw (Mg alloy implant)를 beagle dog의 fractures of zygoma 에 이식한 후 implants의 biocompatibility와 efficiency를 평가하는 것이다.

방법: Beagle dog 의 관골 골절 (zygomatic arch fracture)에 plate와 screw를 fixation 한 후 fracture healing, degradation and bone formation 을 mechanical test, micro CT, 조직형태학적 검사, 조직병리학적 검사 등 분석방법으로 평가하고 생분해성 마그네슘 합금 임플란트와 PLLA 임플란트를 비교하였다.

결과: 두 그룹에서 모두 26주까지 fracture line이 잘 고정 되여 있었으며 염증 반응은 모든 동물에서 유의하게 증가하지 않았다. 조직형태학 분석 결과에서 Mg alloy group이 대조군 인 PLLA group보다 normalized bone area(%)와 normalized void area(%)가 통계적으로 유의하게 더 높았다. Micro-CT 검사에서도 Mg alloy group에서 임플란트 주변의 void area가 대조군 보다 26주까지 더 많은 것을 보여 주었다. 또한 마그네슘 임플란트 주변의 수소 가스는 4 주, 12 주에 증가하다가 26 주에 일정한 감소를 보였다. Ultimate load는 Mg alloy group에서 4주때에 대조군 보다 유의하게 더 높은 강성 및 구조적 강성을 나타냈으며 12주 및 26주때에

도 강성과 구조적 강성은 유지되였다. 조직 병리학 적 분석에서 osteoclast 는 임플란트 고정 후 4주때에 PLLA 군보다 Mg alloy group에서 유의하게 높았다. 26주 때에는 osteoblast와 neovascularization도 Mg alloy group이 PLLA group보다 통계적으로 유의하게 많았다.

결론: 수술 4주 후 마그네슘 합금이 대조군 보다 높은 강도를 나타냈고 12주와 26주때에는 두 군 사이에 유의한 차이는 없었다. 조직학적 분석 데이터를 바탕으로, 마그네슘 합금이 골재생에 기여한다고 여겨진다. 이 결과는 인간의 craniofacial fixation을 위한 마그네슘 합금 plate와 screw의 향후 개발 가능성을 보여준다. 그러나 마그네슘 합금의 부식 속도는 최적화된 조절이 필요할 것으로 생각된다.

주요 단어: 비글견, 관골 골절, 마그네슘 합금 임플란트, 생분해성 임플란트